

Thermal Parameter Estimation Using Recursive Identification

Gary L. Skibinski and William A. Sethares, *Member, IEEE*

Abstract—A novel method that converts a semiconductor transient thermal impedance curve (TTIC) into an equivalent thermal RC network model is presented. Thermal resistance (R) and thermal capacitance (C) parameters of the model are identified using manufacturer's data and off line recursive least square (RLS) techniques. Relevant estimation theory concepts and the formulation of an appropriate model for the identification process are given. Model synthesis is illustrated using an isolated base power transistor module. The application of time decoupled theory for high order thermal models is outlined. Simulation of junction temperature responses using model and manufacturer TTIC's are compared. Estimated parameter validity is further confirmed by parameter calculation obtained from module physical dimensions.

I. INTRODUCTION

POWER converter manufacturers typically utilize the relatively low but significant thermal heat capacity of power semiconductors to obtain short duration overload ratings well in excess of continuous ratings. The methods for determining the peak allowable junction temperature $\{T_j(\max)\}$ under transient and intermittent loading are well established and have remained essentially unchanged since 1959 [1]. The standard approach uses the TTIC supplied by device manufacturers (Fig. 1(a)). Junction temperature response to device power pulses are estimated from this curve and the principle of superposition for conditions such as single pulse overload, repetitive pulse overload, overloads following continuous duty and irregularly shaped power versus time profiles. Indeed, power transistor safe operating area (SOA) limits are usually based upon this approach [2]–[5]. However, transient junction temperature estimation using the TTIC approach has several shortcomings.

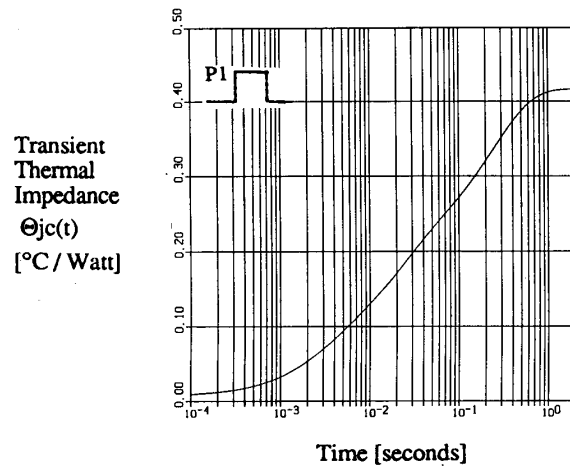
1) *a-posteriori* Calculations: Circuit simulation programs containing sophisticated device models exist that can calculate instantaneous power versus time profiles [6]–[7]. However, instantaneous junction temperature vs. time profiles cannot be solved with the TTIC concept until the entire overload simulation process is complete, stored in memory and broken down into equivalent pulse amplitude and durations. This inefficiency suggests the use of a device thermal model (Fig. 1(b) and (c)) for maximizing simulation capability by solving both the electrical and thermal network models simultaneously.

2) *Graphical Analysis*: The standard TTIC approach requires cumbersome graphical analysis to transform the irregularly shaped power profiles, such as the switching and conduction loss profiles in SOA calculations, into equivalent energy [W-s] square power pulses upon which this curve is based.

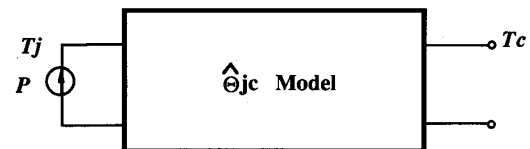
Manuscript received July 23, 1990.

The authors are with the University of Wisconsin-Madison, 1415 Johnson Drive, Madison, WI 53706.

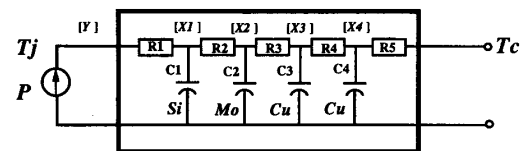
IEEE Log Number 9042335.



(a)



(b)



(c)

Fig. 1. (a) Semiconductor transient Thermal Impedance curve (junction-case). (b) Estimated Black Box Model of Fig. 1(a). (c) Thermal Model Structure of Fig. 1(a) and (b).

3) *Repeat Calculations*: Each application of a new overload sequence requires T_j to be recalculated.

4) *Desired Accuracy*: The accuracy of estimated junction temperatures decreases for increasingly complex overload waveforms such as pulse width modulation (PWM) acceleration of a motor. When using the standard approach, gross simplifying assumptions are necessary to keep graphical analysis and hand computations tractable.

The shortcomings of the standard approach suggest the need to develop an accurate thermal model to make better estimates of T_j . Use of a device thermal model for indirect measurement of the junction to case temperature rise $\{\Delta T_{jc}\}$ may result in improved converter fault diagnostics. Indirectly calculating ΔT_{jc} in real time may be done with the discrete transfer function model of Fig. 1(b) and a Digital Signal Processor (DSP)/microprocessor or an analog operational amplifier model of Fig. 1(c). In addition, potential advantages in substantially increased converter overload ratings exist when using the ΔT_{jc} observer based model in real time adaptive control [8].

In this paper, a new approach to the problem of determining device thermal characteristics is presented from the system identification point of view [9]. Sections II and III outline the basic identification procedure used and the governing laws for device thermal model building. Sections IV and V review and apply estimation theory principles to determine the RC parameter values given the manufacturer's TTIC curve. Section VI presents identification results for an isolated base transistor model example and discusses parameter accuracy of the identified RC values.

II. IDENTIFICATION PROCEDURE

The success or failure of any application of system identification rests on finding an algorithm that can intelligently utilize *a priori* information. The thermal estimation problem has three main features which can be exploited. First, the structure of Fig. 1(c) is known from physical grounds to closely model the thermal behavior of the system, even though the exact values of the R 's and C 's are unknown. This suggests that one of the parametric identification methods should be applicable. The second feature is the TTIC curve, which can be used to construct simulated input/output pairs to sufficiently excite the identification procedure. The third feature is that the thermal time constants have a wide time scale separation. In many identification setups, this would be a serious problem because it is difficult to excite all modes of the system without an inordinately large number of time steps. Since this time scale separation is known to exist *a priori*, however, we are able to exploit it by identifying the slow and fast modes separately via a time decoupling approach. Fig. 2 defines the four basic steps used [10].

1) *Model Formulation*: The type and order of the thermal model structure are defined from *a priori* knowledge about the semiconductor. Some numerical constants of the model can also be obtained *a priori* by applying Newton's Law of Cooling. Discrete state space equations are derived based upon the physical model.

2) *Design of Experiment*: The input signal, sampling interval and experiment length are chosen so that appropriate modes of the thermal model are sufficiently excited for identification.

3) *Parameter Estimation*: This step determines the numerical values of the model structure. The choice of algorithm is the off-line direct method of recursive least squares (RLS). The method shown in Fig. 3 is based upon the fact that the collected output responses are linearly dependent on the unknown parameters where

- k Discrete sampling time
- $u(k)$ Input power pulse sequence into the device.
- $y(k)$ Calculated junction-case temperature response, $T_{jc}(k)$
- $\hat{y}(k)$ Estimated junction-case temperature response, $\hat{T}_{jc}(k)$

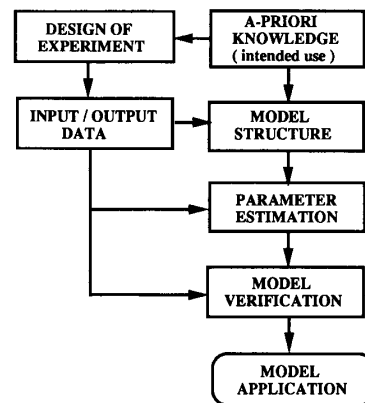


Fig. 2. Identification procedure.

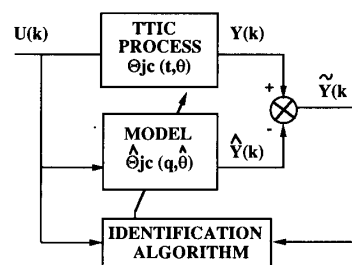


Fig. 3. Parameter estimation technique.

$\tilde{y}(k)$ Output error equation between true $T_{jc}(k)$ and estimated $\hat{T}_{jc}(k)$ responses.

The basic scheme is to use a well planned input power sequence which has a sampling interval shorter than the fastest time constant and an experiment length that is longer than the slowest estimated time constant of the thermal model. True junction temperature response, $T_{jc}(k)$, to $u(k)$ is calculated using the manufacturer's TTIC. The same input test signal is also applied, restarting at $t = 0$, to the $\hat{\Theta}_{jc}$ model and $\hat{y}(k)$ is calculated for each time instant k . The RLS algorithm attempts to drive the $\tilde{y}(k)$ error to zero at each k by adapting the unknown parameters $\hat{\Theta}_{jc}$. The estimated numerator and denominator coefficients of $\hat{\Theta}_{jc}$ converge to steady state values for a properly designed input test signal. The actual resistance and capacitance values may then be determined from these coefficients using the initial model equations formulated.

4) *Model Verification*: This step relates the identification (ID) results to well known physical results. Comparison of $T_{jc}(k)$ versus $\hat{T}_{jc}(k)$ and manufacturer's TTIC versus an estimated TTIC curve are made. Additionally, identified R and C model parameters are compared to calculated RC values obtained from measurements of an actual semiconductor. These four steps are now examined in more detail.

III. MODEL FORMULATION

Transient Thermal Impedance Curve

The semiconductor thermal model structure is implicitly contained in the TTIC as a complex sum of RC exponentials. It is therefore desirable to review the definition, derivation, assump-

tions and application of this curve. The concept of thermal resistance is based upon an analogy between electrical and thermal systems with temperature [$^{\circ}\text{C}$], heat flow due to power dissipation [watts] and thermal resistance [$^{\circ}\text{C}/\text{W}$] being analogous to voltage, current and electrical resistance [11]. The TTIC in Fig. 1(a) is obtained by applying a single square power pulse P_1 to the device until the junction temperature reaches steady state at time t_{ss} . Junction temperature rise $\{\Delta T_{jc}\}$ is determined by fixing the case constant at ambient temperature $\{T_c = T_a\}$ and measuring device temperature with infrared methods or electrical temperature sensitive parameters $\{\text{TSP}\}$ such as forward voltage drop $\{V_f\}$ or base emitter voltage $\{V_{be}\}$ [12]. The actual ΔT_{jc} rise is found by correlating the measured change in V_{be} ($\cong 2 \text{ mV}/^{\circ}\text{C}/\text{junction}$) versus time to a previous calibrated V_{be} versus temperature test for constant T_a and base current. The transient thermal impedance is defined at any time t as

$$\Theta_{jc}(t) = \frac{T_j(t) - T_c(t)}{P_1} = \frac{\Delta T_{jc}(t)}{P_1}. \quad (1)$$

The thermal system is assumed to be linear, and hence superposition can be applied to the TTIC. The TTIC is a step response curve with zero initial conditions, relating device step input power to ΔT_{jc} at the output. The power profile in Fig. 4(a) can be separated into equivalent heating and cooling pulse durations of t_x and t_y as shown in Fig. 4(b). The junction temperature rise can be determined by adding individual T_{jc} pulse responses [1]:

$$\Delta T_{jc}(t_1) = P_1 * \Theta_{jc}(t_1) \quad (2)$$

$$\Delta T_{jc}(t_2) = P_1 * \Theta_{jc}(t_2) - P_1 * \Theta_{jc}(t_2 - t_1) + P_2 * \Theta_{jc}(t_2 - t_1). \quad (3)$$

The published TTIC is usually higher than the tested value to account for manufacturing variations and the increase in thermal resistance over time.

a-priori Knowledge

Knowledge of the physical properties of the semiconductor can be used to fix the model structure and order, and to determine some numerical values of the Black Box shown in Fig. 1(c). The use of all available *a priori* knowledge prior to application of the identification algorithm is important since misleading results due to an assumed wrong structure are difficult to detect from data alone. Also, *a priori* knowledge can enhance model validity and model accuracy. An appropriate model can be formulated using 1) physical knowledge, 2) I/O measurements, or both.

1) *Physical Knowledge*: The model order is dependent on the type of semiconductor package used as shown in Fig. 5. The exact order can be determined by visual inspection of the package cross sectional view and replacing significant heat capacity materials (Cu , Si , Mo) with thermal capacitances. The number of capacitors determines the model order. One dimensional heat flow from junction to case results in the typical RC network structure shown in Fig. 1(c). Numerical values for R_5 and C_4 of the copper base can be obtained without package disassembly by applying the governing thermal laws defined in Appendix I to a 4th order 50-A isolated base transistor:

$$R_i = L_i / (K * Ae) \quad [^{\circ}\text{C}/\text{W}] \quad (4)$$

$$C_i = \rho * Cp * V \quad [\text{W}\cdot\text{S}/^{\circ}\text{C}]. \quad (5)$$

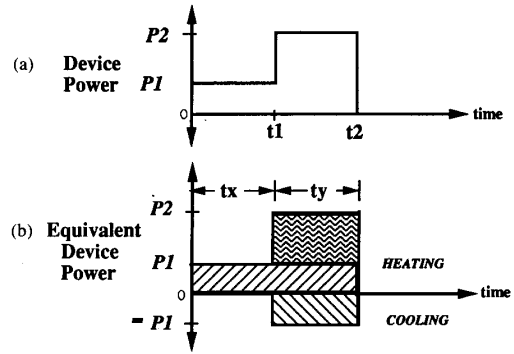


Fig. 4. (a) Device power profile versus time. (b) Equivalent heating and cooling pulses.

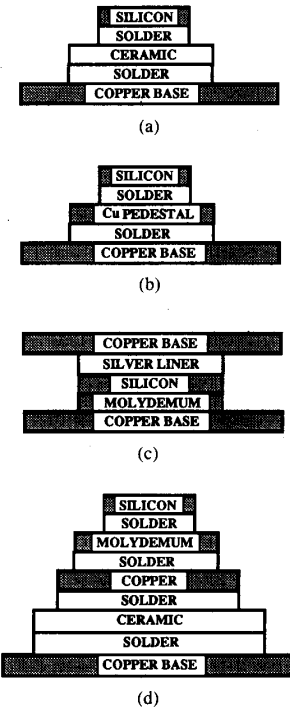


Fig. 5. Model order dependent on semiconductor package. (a) Direct bonded copper process [2nd order]. (b) TO3/TO220/stud type [3rd order]. (c) Compression bonded thyristor [4th order]. (d) Isolated base transistor module [4th order].

Thermal resistance and capacitance calculations can be extended to R_1 – R_4 and C_1 – C_3 by disassembling the package and physically measuring each material thickness and cross section area perpendicular to heat flow. This calculated parameter approach is documented in Appendix I with the results shown in Table I. An analog simulation of this RC structure is plotted in Fig. 6 versus the actual TTIC. This procedure alone may produce sufficient $\Theta_{jc}(t)$ accuracy for the intended use of the model.

2) *I/O Measurement*: The asymptotic behavior at the origin and steady state time t_{ss} of the manufacturer's TTIC in Fig. 6 can provide numerical values for parameters R_1 , C_1 and for the

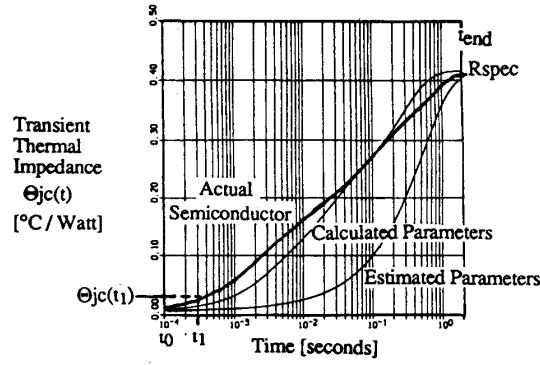


Fig. 6. Transient thermal impedance curves.

TABLE I
CALCULATED AND ESTIMATED RC PARAMETERS

	R1	R2	R3	R4	R5	C1	C2	C3	C4
Calculated	0.006	0.111	0.122	0.166	0.011	0.033	0.148	1.180	9.500
Estimated	0.008	0.022	0.078	0.291	0.011	0.360	0.488	0.665	0.900

sum of $R1$ through $R5$ in Fig. 1(c). The horizontal asymptote at the origin reflects the silicon thermal resistance $R1$. The initial slope near the origin of Fig. 6 can be silicon thermal capacity by the analogy to $i = C/(dv/dt)$:

$$\text{Power} \cong C1 \Delta T_{jc} [\text{°C}]/\Delta \text{Time [s]} \quad [\text{W}] \quad (6)$$

$$C1 \cong P * (t_1 - t_0) / P * (\theta(t_1) - \theta(t_0)) \quad [\text{W-S/°C}] \quad (7)$$

The sum of $R1$ – $R5$ is the dc gain of the mathematical transfer function model and is the value $\theta_{jc}(t_{ss})$ read from the TTIC.

$\hat{\theta}_i$ Parameter Initialization Procedure

As an alternative to the physical RC calculation procedure above, the following procedure may be used to find initial estimates for the RLS identification algorithm using only TTIC information. Although this method involves crude approximations, it is helpful in estimating the model time constants for selecting a suitable RLS sampling time and providing parameters sufficiently close to the actual so that the RLS routine converges rapidly.

The following known data in (8a–d) can be obtained from the manufacturer's data specification sheet, the TTIC of Fig. 6 or from external physical dimensions:

$$R_{spec} = (R1 + R2 + R3 + R4) + R5 \quad (8a)$$

$$R5 \text{ is calculable from baseplate case thickness dimensions} \quad (8b)$$

$$R1 \text{ is from the TTIC as in the previous section} \quad (8c)$$

$$\tau_4 \text{ is from the TTIC since } t_{end} \text{ is known and is } 5t_4. \quad (8d)$$

Crude approximations for a $n = 4$ th order system are

$$t_{end} \cong [5\tau_4] \cong 5[(R1 + R2 + R3 + R4)]C4 \quad (8e)$$

$$\tau_4 \cong [5\tau_3] \cong 5[(R1 + R2 + R3)]C3 \quad (8f)$$

$$\tau_3 \cong [5\tau_2] \cong 5[(R1 + R2)]C2 \quad (8g)$$

$$\tau_2 \cong [5\tau_1] \cong 5[(R1 * C1)] \quad (8h)$$

$$\tau_1 \cong [R1 * C1] \cong [t_{end}/5^n]. \quad (8i)$$

Thermal capacitance is assumed to be increasing by a constant factor MF_i from one stage to the next:

$$C2 \cong MF_1 * C1 \quad (8j)$$

$$C3 \cong MF_2 * C2 \quad (8k)$$

$$C4 \cong MF_3 * C3 \quad (8l)$$

$$C4/C1 \cong MF_1 * MF_2 * MF_3 \quad (8m)$$

$$MF_i \cong (C4/C1)^{1/3}. \quad (8n)$$

Parameter $C4$ is found using (8a), (8b), (8d), and (8e). Capacitor $C1$ is found using (8c) and (8i). Capacitors $C2$ and $C3$ are extracted from (8j), (8k), and (8n). Resistor $R4$ is found by solving for the $\{R1 + R2 + R3\}$ sum of (8f) and substituting into (8e). Resistor $R3$ is found by solving for the sum $\{R1 + R2\}$ of (8g) and substituting into (8f). Resistor $R2$ is calculated directly from (8g). Table I summarizes the Estimated RC parameter results for the known data shown below.

$$t_{end} = 1.8 \text{ s} \quad R_{spec} = 0.41 [\text{°C/W}]$$

$$R1 = 0.008 [\text{°C/W}] \quad R5 = 0.0106 [\text{°C/W}]$$

Assumptions

The thermal model for Fig. 1 and Fig. 5 is assumed to be a linear, n th order lumped parameter, time invariant, deterministic, single input single output (SISO) system. Nonlinear radiation effects which are proportional to the 4th power of temperature are not significant since one dimensional heat flow is mostly by conduction. However, silicon conductivity is nonlinear with temperature varying 2:1 over the 25–150°C operating range and may effect the estimates of the $R1$ and $R2$

thermal resistances. Also, some insulators such as BeO will vary by 20% over the same range. The present procedure ignores these nonlinearities, though their incorporation into the design procedure is an important area for further investigation. Lastly, measurement noises are assumed negligible.

Equations

A thermal model can be formulated using either an internal state space or I/O transfer function model approach. The first method is the most desirable since it is directly related to the physical structure of Fig. 1(c). However, the need to measure the internal states (x_1, x_2, x_3, x_4) to find model coefficients precludes its use. The transfer function approach must be used since only I/O data from the TTIC is available. The disadvantage of this approach is that the Θ_{jc} model coefficients obtained from I/O data have no direct physical meaning. The RC parameters of the structure are hidden in the numerator and denominator coefficients and must be further extracted. The transfer function model is developed in the continuous time domain and must be further discretized for use in the identification algorithm.

Continuous State Space Model

The system equations for the 4th order structure in Fig. 1(c) can be obtained using the capacitor voltages (temperatures) as the state variables (x_1, x_2, x_3, x_4). The output equation variable (Y) represents the silicon absolute junction temperature T_j . The input variable (u) represents the device power in watts. The transfer function $\hat{\Theta}_{jc}$ reflects the temperature rise for a given power input. It is derived by applying the Laplace transform operator $\{s\}$ to (9a), solving for X and substituting into (10a):

$$\dot{X} = AX + Bu \quad [^\circ\text{C}/\Delta t] \quad (9a)$$

$$Y = CX + Du \quad [^\circ\text{C}] \quad (10a)$$

$$Y/u = C(sI - A)^{-1}B + D \quad [^\circ\text{C}/\text{W}] \quad (11a)$$

where $B = (1/C1, 0, 0, 0)^T$, $C = (1, 0, 0, 0)^T$, $D = R_1$, and

$$A = \begin{bmatrix} \frac{-1}{R2C1} & \frac{1}{R2C1} & 0 & 0 \\ \frac{-1}{R2C2} \left(\frac{-1}{R2C2} - \frac{1}{R3C2} \right) & \frac{1}{R3C2} & 0 & 0 \\ 0 & \frac{1}{R3C3} & \left(\frac{-1}{R3C3} - \frac{1}{R4C3} \right) & \frac{1}{R4C3} \\ 0 & 0 & \frac{-1}{R4C4} & \left(\frac{-1}{R4C4} - \frac{1}{R5C4} \right) \end{bmatrix}$$

The symbolic transfer function corresponding to (11) contains four numerator and four denominator coefficients in the s^0 to s^4 powers. Determination of the RC parameter values requires simultaneously solving the eight coefficient equations. Four of the eight coefficients each contain 21 nonlinear sum and product terms of the form $1/(R_i C_j)$, which makes solution a formidable task. Using the *a priori* knowledge that the values of the capacitors are widely separated in this 4th order thermal model,

the above equation can be split into two cascaded 2nd order systems which match the dc gain and overall dynamics of the original system. Thus, only simpler 2nd order equations need be developed using $x_1, x_2, R1, R2, R3, C1$ and $C2$:

$$\begin{pmatrix} \dot{x}_1 \\ \dot{x}_2 \end{pmatrix} = \begin{pmatrix} \frac{-1}{R2C1} & \frac{1}{R2C1} \\ \frac{-1}{R2C2} & \frac{-1}{R2C2} - \frac{1}{R3C2} \end{pmatrix} \begin{pmatrix} x_1 \\ x_2 \end{pmatrix} + \begin{pmatrix} \frac{1}{C1} \\ 0 \end{pmatrix} P \quad (12)$$

$$Y = [1 \ 0]X^T + [R1]P. \quad (13)$$

This is the time scale decoupling, and is possible whenever the unknown system has widely separated modes. In essence, the identification of the slow modes is conducted separately from the identification of the fast modes.

Discrete Transfer Function Model

In order to utilize an appropriate identification algorithm, the continuous system (12) and (13) must be discretized for computer implementation. There are several possible methods such as Eulers methods, Tustins approximation, step invariance, etc. An infinite series approximation was chosen because it leads to relatively simple equations relating the RC parameters to the filter coefficients. The discrete system equations are defined using the time shift operator, $\{q\}$.

$$X(k+1) = qX(k) = \Phi X(k) + \Gamma u(k) \quad [^\circ\text{C}/\Delta t] \quad (14)$$

$$Y(k) = CX(k) + Du(k) \quad [^\circ\text{C}] \quad (15)$$

The pulse transfer function is derived by solving (14) for $x(k)$ and substituting into (15) [13]:

$$\hat{\Theta}_{jc}(k) = Y(k)/u(k) = C(qI - \Phi)^{-1}\Gamma + D \quad [^\circ\text{C}/\text{W}] \quad (16)$$

where

h = sample interval

Φ = state transition matrix

$\hat{\Phi} = e^{Ah} = I + Ah$ {first order approximation}

$$\Gamma = \int_0^h e^{A\xi} d\xi B. \quad (17)$$

Performing the matrix operations and applying the backward shift operator (q^{-1}) yields the standard digital filter format with the coefficients defined in Appendix II:

$$\hat{\Theta}j_c(q, \hat{\theta}) = \hat{H}(q, \hat{\theta}) = \begin{pmatrix} b_0 + b_1q^{-1} + b_2q^{-2} \\ 1 + a_1q^{-1} + a_2q^{-2} \end{pmatrix} \quad (18)$$

where

$$\hat{\theta} = [a_1, a_2, b_0, b_1, b_2]^T$$

$$n = \text{order of the numerator} = 2$$

$$m = \text{order of the denominator} = 2.$$

The linear difference equation for the system is

$$y(k) = a_1y(k-1) + a_2y(k-2) + b_0u(k) + b_1u(k-1) + b_2u(k-2). \quad (19)$$

Discretization Error

Substitution of $q = 1$ into (18) provides an estimate for the discretization error due to a first order approximation for the state transition matrix:

$$\hat{\Theta}j_c(1, \hat{\theta}) = \hat{H}(1, \hat{\theta}) = \|R_1 + R_2 + R_3\| - \{0.5h/C_1\}. \quad (20)$$

The first term is the correct dc gain of the 2nd order system while the second term is due to the $O(h^3)$ error defined in Appendix II. This term is negligible for small sample times used in identifying the fast time constants but can lead to large dc gain errors ($\cong 30\%$) in $y(k)$ for large sample time $\{h\}$. This is further detailed in Section VI.

Parameter Error Estimation

A worst case steady state error bound estimate for parameter R_1 due to (20) can be derived using the standard rule of thumb that the system is sampled $10\times$ faster than the fastest time constant to be identified.

$$\{h * 0.5/C_1\} = \begin{pmatrix} \tau_{\text{fastest}} \\ 10 \end{pmatrix} \begin{pmatrix} 0.5 \\ C_1 \end{pmatrix} = \begin{pmatrix} R_1C_1 \\ 20C_1 \end{pmatrix} = \pm 5\% \|R_1\|. \quad (21)$$

RC Parameter Extraction from Filter Coefficients

The five RC parameters may be found by simultaneously solving the five coefficient equations in Appendix II. A convergent solution is obtained if the $O(h^3)$ error term in the b_2 equation is eliminated before solving. The parameter solution equations [22]–[26] must be solved in the sequential order as shown. These equations were solved by hand using the variable substitution method and verified using the symbolic equation solver *Mathematica* [14].

$$R_1 = b_0 \quad (22)$$

$$C_1 = ha_1 / \{b_0[(a_1 - a_2) + (b_2 - b_1)/b_0]\} \quad (23)$$

$$R_2 = (-0.5)h^2 / \{b_0C_1^2[(b_1/b_0) - a_1] - C_1h\} \quad (24)$$

$$C_2 = h / \{R_2\{[a_1 + 2.0 - (h/R_2C_1)] - (a_1 + a_2 + 1.0)(R_2C_1/h)\}\} \quad (25)$$

$$R_3 = h^2 / \{C_1C_2R_2(a_1 + a_2 + 1.0)\}. \quad (26)$$

IV. DESIGN OF THE EXPERIMENT

Standard Identification Procedure

In the semiconductor thermal model structure of Fig. 1(c), the time constants (τ_i) cover a 1500:1 range from μsec to seconds. Identifying these major time constants by standard identification methodology requires multiple trial & error ID applications, since coefficient accuracy tends to degenerate for systems with τ 's having more than two decades of time separation. Such experiments to identify the τ 's require engineering tradeoffs regarding sampling time $[T_s]$, experiment record length, and input signal amplitude. Proper identification of the fast time constant requires a high sampling rate, identification of the slow time constant requires a long record of input/output data. Together, these imply a cumbersome and poorly conditioned identification setup. One approach is to collect a number of experiments and to average them to obtain an averaged transfer function model that drives the $y(k) - \hat{y}(k)$ error to zero for a specific time region of interest. Further, ambiguous sets of RC parameters may result if the RC extraction procedure of Section III is applied to such averaged models.

Proposed Time Decoupled Theory (TDT)

The disadvantages of widely separated time constants can be circumvented since we know *a priori* that such a separation exists. The basic strategy of time decoupled identification is to run two separate identification procedures, one for the slow modes and one for the fast modes. Besides the advantages of tailoring the sampling rates and record lengths to the expected order of magnitude of the time constant, this decoupling allows a simpler RC parameter extraction procedure. Fig. 7 conveys the TDT procedure as applied to the 4th order semiconductor module example. The 4th order model is decoupled into two independent 2nd order systems. The split model is reasonable given the analogous electrical model where a high frequency device power sequence of short experiment length will charge C_1 and C_2 while leaving C_3 and C_4 virtually unchanged. Similarly, the fast modes will be virtually invisible to a step inputs with a slow sampling rate. The basic TDT concept involves using multiple identification runs to estimate the four major time constants in succession from the fastest to the slowest.

The fastest time constant $[\tau_1]$ of Fig. 7a is identified by suitable selection of 1) a sampling rate that is fast enough for the estimated $[\tau_1]$ to be identified, 2) a persistently exciting device power sequence, 3) an experiment record length long enough to allow for parameter convergence and 4) using all available *a priori* knowledge for R_1, R_2, R_3, C_1 and C_2 initial estimates. True junction temperature $y(k)$ is calculated using the TTIC. The identified a_i and b_i coefficients will typically converge in less than $k = 15$ samples. The $\hat{\theta}_i$ parameters are then passed to the RC extraction procedure. The newly updated values for R_1 and C_1 will be very close to the actual values while $R_2, R_3,$ and C_2 values will be relatively inaccurate.

The ID procedure is next repeated using the RC parameters from the previous run as initial *a priori* estimates. The sampling

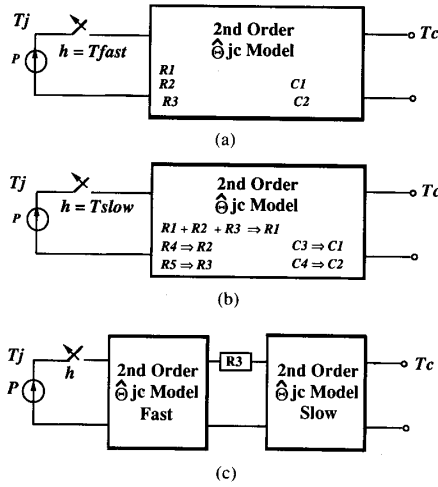


Fig. 7. Time decoupled theory procedure (TDT). (a) Identifying the fast τ 's. (b) Identifying the slow τ 's. (c) Connecting the split models.

rate is now chosen to be greater than Ts_1 but still fast enough to identify the second guess-timated time constant τ_2 . Application of the ID algorithm and parameter extraction procedures will modify R_2 , R_3 and C_2 to the correct actual values while the faster R_1 - C_1 parameters will remain unchanged.

To identify the slower time constants [τ_3 and τ_4], the split model of Fig. 7(b) is used with the same second order equations as was used in Fig. 7(a). A key parameter change is the substitution of $\{R_1 + R_2 + R_3\} = R_1$ to maintain the TTIC overall dc gain and slower system dynamics. The sampling rate is selectively increased and the ID and RC extraction procedures are similarly repeated to find R_4 , R_5 , C_3 , and C_4 in about two or three ID runs. Some systems may require repeating this fast/slow identification procedure to more accurately identify the interconnecting R_3 element in Fig. 7(c). Considerations for choosing a suitable sampling rate, experiment length and input signal amplitude are now discussed in more detail.

Input Signal

The amplitude of the device input power signal should be as high as allowable to improve accuracy. The form of the input signal should: 1) consist of square pulses so that the TTIC curve for $y(k)$ calculation may be directly used, 2) have a random amplitude versus time profile to allow ID convergence to a unique set of parameter values, 3) never have a non-realistic negative power pulse, 4) ideally result in rated T_j for rated power $\{\text{Prated}\}$ with steady state thermal resistance at $T_c = 25$ C. These constraints are met by taking a pseudo random sequence consisting of the first positive 50 digits of pi (0-9). For long sequences, the average random digit value approaches 5. The $u(k)$ amplitude equation used is

$$u(k) = 2.0 * \text{Prated} * \{\text{Random digit}\} / 10. \quad (27)$$

To help identify longer term dynamics, six similar amplitude pulses {e.g., $u(1)$ to $u(6)$ } were grouped together before the next allowable amplitude change.

Sampling Time

The Nyquist theorem determines the minimum sampling rate to use for each ID run. A commonly used practical rule of thumb

is to sample $10 \times$ faster than the fastest time constant to be identified:

$$h = \tau_{\text{smallest}} / 10 \quad (28)$$

Experiment Length

Parameter accuracy is dependent on the record length so that a sufficient amount of data points is available to give long term dynamics. The RLS parameters theoretically converge in $\cong (n + m)$ steps for a white noise input [15]. For the random step input sequence, four to 15 sample intervals were typically observed for $\hat{\theta}_i$ -parameters to converge.

$$\{k\} \text{ length} \cong (4 \text{ to } 15) * h. \quad (29)$$

Test Case

To verify the accuracy of the collected ID parameters, an analog ACSL [16] simulation of the RC parameters for a single step input power pulse is done to compare the final estimated and actual TTIC.

A test case utilizing the calculated transistor thermal parameters of Tables III and IV was used to verify the TDT procedure. As a first step, the linear difference equation (19) was used to calculate the true $y(k)$ rather than the actual TTIC. The final results are found in Section VI.

V. PARAMETER ESTIMATION

Method

The goal of the identifier block in Fig. 3 is to determine unknown a_i and b_i filter coefficients of the parameter vector $\hat{\theta}$ in $\hat{\theta}_{jc}(q, \hat{\theta})$. Deriving a control law for parameter estimation from the parameter vector error $[\theta_i - \hat{\theta}_i]$ is not possible since $\hat{\theta}_i$ parameters are not directly measurable. However, a prediction estimate $\hat{y}(k)$ for every measurable/calculable $y(k)$ can be formulated. If a linear model is assumed, then the resulting prediction error estimate $[y(k) - \hat{y}(k)]$ is a function of θ as shown in (19):

$$\text{error}(k, \hat{\theta}) = y(k) - \hat{y}(k). \quad (30)$$

Various methods that minimize the sum of the squares of this prediction error are maximum likelihood, least mean squares, extended least squares and recursive least squares. The RLS method was chosen since it is computationally fast, requires no matrix inversions, and tends to converge rapidly. Observed convergence rates for the 2nd order model varied from four to eight amplitude step changes, depending on the closeness of the $\hat{\theta}_i$ initial guesses. Thus, only a small number of $y(k)$ calculations using the TTIC are required. A disadvantage of RLS is the $\hat{\theta}_i$ biasing toward wrong values as $k \rightarrow \infty$ when the process output $y(k)$ is measured in the presence of noise. However, in this application, $y(k)$ is virtually noiseless since the primary source of noise appears to be interpolation errors when reading the TTIC curve.

Solution

A recursive identifier is one in which both input $u(k)$ from $\{k = 0 \text{ to } N - 1\}$ and output $y(k)$ measurements from $\{k = 1 \text{ to } N\}$ are made and input to the estimator to determine the parameter vector $\hat{\theta}$. The symbol N is the total number of sampling intervals over which the data is collected. The minimization process requires $N > n + m$ to effectively average out error residuals.

Defining the data regression vector as (31), then the error at any given time $k = \eta$ as a function of $\hat{\theta}$ is given by (32):

$$\chi(k+1) = \begin{bmatrix} y(k) \\ \vdots \\ y(k+1-n) \\ u(k) \\ \vdots \\ u(k+1-m) \end{bmatrix} \quad (31)$$

$$\text{error}(\eta, \hat{\theta}) = y(\eta) - \chi^T(\eta)\hat{\theta} \quad (32)$$

The error vector equation and the error vector, output vector and regression vectors collected from time η to N is thus:

$$\epsilon(N, \hat{\theta}) = Y(N) - \Psi(N)\hat{\theta} \quad (33)$$

where

$$\epsilon(N, \hat{\theta}) = \begin{pmatrix} e(\eta, \hat{\theta}) \\ e(\eta+1, \hat{\theta}) \\ \vdots \\ e(N, \hat{\theta}) \end{pmatrix} \quad Y(N) = \begin{pmatrix} y(\eta) \\ \vdots \\ y(\eta+1) \\ y(N) \end{pmatrix}$$

$\in \mathbb{R}^{N-\eta+1}$ $\in \mathbb{R}^{(N-\eta+1) \times (n+m+1)}$

$$\Psi(N) = \begin{pmatrix} \chi^T(\eta) \\ \chi^T(\eta+1) \\ \vdots \\ \chi^T(N) \end{pmatrix}$$

$\in \mathbb{R}^{(N-\eta+1) \times (n+m+1)}$

The optimal $\hat{\theta}$ is the one that minimizes (33) error in a least square sense. This requires a performance index $J(N, \hat{\theta})$ taking the gradient $\partial J/\partial \hat{\theta}$, and setting it equal to zero. This results in the well known least square solution of (35), [15]:

$$J(\eta, N, \hat{\theta}) = \sum_{k=\eta}^N \epsilon(k, \hat{\theta}) \epsilon(k, \hat{\theta}) \quad (34)$$

$$\hat{\theta}[N] = [\Psi(N) \Psi(N)]^{-1} \Psi^T(N) Y(N) = P[N] Y[N] \quad (35)$$

$$\hat{\theta}[N+1] = P[N+1] Y[N]. \quad (36)$$

The optimal coefficients $\hat{\theta}$ will exist if the pseudoinverse $P[N]$ is nonsingular. This condition is satisfied assuming persistent excitation, which is guaranteed by selecting the amplitude of $u(k)$ randomly for times up to $k = N$ by using a pseudo random sequence. As new data arrives $\{u(N), y(N+1)\}$, the objective of RLS is to update $\hat{\theta}[N]$ to $\hat{\theta}[N+1]$ in terms of the old data and $\hat{\theta}[N]$ vector and similarly update $P[N]$ to $P[N+1]$. The $P[N+1]$ matrix in (36) can be related to $P[N]$ without inversion via the matrix inversion lemma [17]. Thus $\hat{\theta}[N+1]$ can be related to $\hat{\theta}[N]$ without inversion by

$$\hat{\theta}(k+1) = \hat{\theta}(k) + L(k+1)[y(k+1) - \chi^T(k+1)\hat{\theta}(k)], \quad (37)$$

new estimate = old estimate + correction term, where

$$L(k+1) = \text{Gain matrix}$$

$$y(k+1) = \text{New data measured}$$

$$\chi^T(k+1)\hat{\theta}(k) = \text{Prediction of } y(k+1)$$

$$\text{correction term} = \text{Gain} * (\text{y output error equation}).$$

Starting Conditions

A first estimate for $\hat{\theta}[N]$ without inversion may be obtained using the *a priori* knowledge of Section III parameter initialization procedure. Alternatively, Soderstrom's suggested starting conditions for $\hat{\theta}[N]$ and $P[N]$ can be utilized. Two initial conditions for $y(k)$ must be calculated for the 2nd order model, thus starting the process at $k = 2$:

$$\hat{\theta}[N] = 0 \quad P[N] = \alpha * I \quad \alpha = (10/n) \sum_{k=0}^1 y^2(k). \quad (38)$$

Algorithm

The identification scheme [18] used for the computer program is

- (0) Initialize $\hat{\theta}[N]$ and $P(N)$; set $k = 2$
- (1) Form $\chi^{(k+1)}$ data vector = $(n+m+1) * 1$ matrix for SISO system
- (2) Update $L(k+1) = [1/\gamma]P(k) \chi(k+1) \{1/a + [\chi^T(k+1)/\gamma]P(k) \chi(k+1)\}^{-1}$
where $\gamma = 1$
 $a = 1$
 $\{\}^{-1}$ = simple inverse of a scalar value
 $L(k+1) = (n+m+1) \times 1$ matrix
 $P(k) = (n+m+1) \times (n+m+1)$ matrix
- $\chi(k+1) = (n+m+1) \times 1$ vector
 $\chi^T(k+1) = 1 \times (n+m+1)$ vector
- (3) Measure $y(k+1), u(k+1)$
- (4) Update $\hat{\theta}(k+1) = \hat{\theta}(k) + L(k+1)[y(k+1) - \chi^T(k+1)\hat{\theta}(k)]$
- (5) Update $P(k+1) = [1/\gamma]\{I - L(k+1) \chi^T(k+1)\} P(k)$
- (6) Replace k by $k+1$ and go to (1).

VI. RESULTS

$y(k)$ Calculation

Calculation of the true junction-case temperature, $\Delta T_{jc} = y(k)$, in the RLS routine must be done using the TTIC and a persistently excited device input power sequence, $u(k)$. The calculated parameter TTIC shown in Fig. 6 was specifically chosen as a test case example since the RC parameters generating this curve are exactly known and can be compared to "Identified" RC parameters. A computer program was written to calculate $y(k)$ utilizing input data points (10 pts/decade) from the test case TTIC curve. The program calculates ΔT_{jc} for a continuous $u(k)$ input sequence using the superposition of equivalent heating and cooling pulses.

Fig. 8 shows a typical $u(k)$ input power sequence and output ΔT_{jc} response for a 4th order ACSL analog simulation model using the RC Calculated Parameters in Table I. The basic $u(k)$ pulse pattern from $t = 0$ to $t = 2.5$ ms was repeated starting at

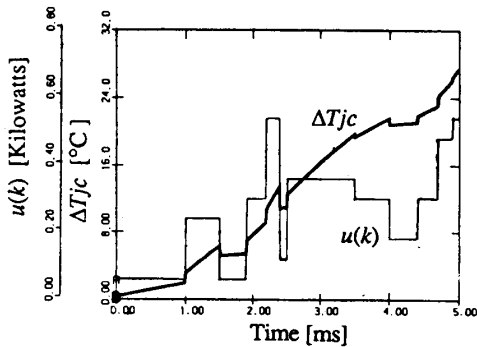


Fig. 8. Simulated analog ΔT_{jc} response to $u(k)$ power sequence.

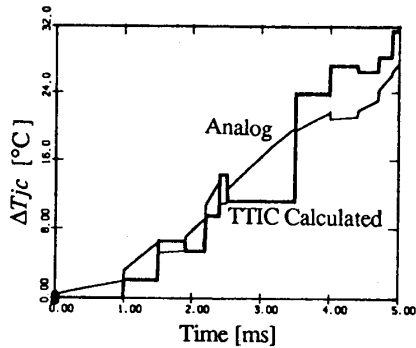


Fig. 9. TTIC calculated and analog ΔT_{jc} responses to $u(k)$.

$t = 2.5$ ms. Of particular interest is the instantaneous temperature jump at each new $u(k)$ pulse due to the $P * R1$ component of Fig. 1(c).

Fig. 9 shows the program TTIC Calculated ΔT_{jc} discrete step response as well as the analog ΔT_{jc} response of Fig. 8. The TTIC inherently incorporates the heating/cooling integration step while providing "sampled" results at the end of each pulse. The discrete TTIC and analog Simulated ΔT_{jc} responses are virtually identical at the end of each pulse from $t = 0$ to $t = 2.5$ ms. At time $t = 2.5$ ms, the TTIC program was restarted, retaining the ΔT_{jc} (2.5 ms) value as a new starting point, and assuming the next pulse from $t = 2.5$ to 3.5 ms is of 1 ms duration. The resulting error that follows between the two ΔT_{jc} responses illustrates a typical misapplication of the TTIC concept that violates the single pulse-zero initial condition assumptions upon which the curve is based. This is further clarified by calculating both analog and TTIC program ΔT_{jc} responses at $t = 2.5$ ms and $t = 3.5$ ms.

The TTIC ΔT_{jc} response is calculated for a single equivalent heating pulse of 2.5 ms duration and an amplitude (165 W) corresponding to the average value of $u(k)$ from $t = 0$ to $t = 2.5$ ms. The resulting temperature using the calculated parameter curve of Fig. 6 is 10.6°C and is in agreement with the actual 11.1°C value obtained with both the TTIC program and analog simulation.

The calculated TTIC ΔT_{jc} response at 3.5 ms cannot be done by restarting at $t = 2.5$ ms as described above. The correct method must assume the device power profile of Fig. 4(a) with $P1 = 165$ W, $P2 = 360$ W, $t1 = 2.5$ ms, and $t2 = 3.5$ ms. Using the TTIC of Fig. 6 and (3) results in less than 0.5°C error from the true temperature.

True RLS $y(k)$ calculation for the test case example with known RC parameters was done using (19) discrete difference equation since it was easier to use and provided discrete temperature information identical to the TTIC computer program.

Test Case Results

Table II results show that only four basic identification runs were needed to identify the nine unknown RC parameters. Correctly identified parameters in Table II are enclosed in a solid box. The four basic time constants listed in the τ_{calc} column are a direct result of the $\hat{\theta}$ parameter initialization procedure using (8e)–(8i) and the actual TTIC of Fig. 6. A suitable sampling rate for each ID run was derived from the τ_{calc} column by applying (28).

The $R1$, $R2$, $R3$, $C1$ and $C2$ values were identified in 2 ID runs using the Fast 2nd order $\hat{\Theta}_{jc}$ model. Run 1a used the Soderstrom starting conditions assuming no *a priori* parameter information. As seen from Table II, $R1$ and $C1$ are properly identified, as expected, for $h = 10 \mu s$. Run 1b shows that additionally $R2$ can be correctly identified by using all the *a priori* initial parameter estimates from Table I. Following the TDT procedure, the output identified parameters from run 1b were used as initial parameter estimates for run 2 using $h = 1.0$ ms. Run 2a results show that the final $R3$ and $C2$ values enclosed by the dashed box in Table II are within 20% of the actual values. This error is due to the method of calculating true $y(k)$ using the linear difference equation rather than the TTIC approach. This is caused by the dc gain discretization error introduced by the $O(h^3)$ term in the b_2 filter coefficient of Appendix II. Run 2b removed this error term resulting in final identified parameters within 0.1% accuracy. Fig. 10 shows a graphical comparison of ID runs 1a, 1b, 2a, and 2b by reconstructing the TTIC from corresponding identified RC parameters.

Components $R3$, $R4$, $R5$, $C3$ and $C4$ were identified using the slow $\hat{\Theta}_{jc}$ model in runs 3 and 4. The initial parameter estimate for $R3$ in run 3 was determined by adding the $R1$, $R2$, and $R3$ values identified from run 2b. The remaining initial parameters were obtained from the $\hat{\theta}$ Initialization procedure and Table I. The results from run 3 show that, similar to run 1b, the $R3$ – $C3$ parameters associated with the faster time constant are correctly identified. Run 4 used these two component values along with estimates for $R4$, $R5$ and $C4$ from Table I as input parameters. The final identified parameters were within 0.2% of the actual values. Figs. 11 and 12 show typical identification waveforms for run 4 with $h = 100$ ms.

Fig. 11 illustrates the output error equation, $\bar{y}(k) = y(k) - \hat{y}(k)$, being driven to zero in $k = 7$ samples. After time $k = 7$, the $y(k)$ and $\hat{y}(k)$ temperature response waveforms to the $u(k)$ sequence are identical. The $u(k)$ power sequence consists of six similar amplitude pulses before changing at $k = 7$. Fig. 12 depicts the same $u(k)$ power sequence applied as in Fig. 11. In addition, a typical RLS convergence pattern for two $\hat{\theta}$ parameter values is shown. The digital filter coefficients, $\hat{\theta}_1 = a_1$ and $\hat{\theta}_3 = b_0$, are shown dynamically adapting to new values to satisfy the $\bar{y}(k)$ error equation and also reach steady state at $k = 7$ samples. The steady state values of the five identified $\hat{\theta}_i$ were used to further extract the model RC parameters.

VIII. CONCLUSION

This paper has identified a need for a device thermal model to maximize simulation capability by solving both the electrical and thermal network models simultaneously. A new approach to the problem of determining device thermal model character-

TABLE II
SUMMARY OF RLS IDENTIFICATION RUNS

ID	Run #	h (ms)	tcalc (ms)	Initial Parameters									Identified Parameters																									
				R1	C1	R2	C2	R3	C3	R4	C4	R5	R1	C1	R2	C2	R3	C3	R4	C4	R5																	
1a	0.01	0.32		0.0000	0.0000	0.0000	0.0000	0.0000	---	---	---	---	---	---	---	---	---	---	---	0.0064	0.0324	0.0179	0.0005	0.0762	---	---	---	---	---	---	---	---	---	---	---	---		
1b	0.01	0.32		0.0080	0.3600	0.0000	0.0220	0.0780	---	---	---	---	---	---	---	---	---	---	---	0.0064	0.0329	0.1095	0.0727	-0.015	---	---	---	---	---	---	---	---	---	---	---	---		
2a	1.0	16		0.0064	0.0329	0.1095	0.0727	-0.015	---	---	---	---	---	---	---	---	---	---	---	0.0064	0.0329	0.1083	0.1697	0.1095	---	---	---	---	---	---	---	---	---	---	---	---	---	
2b	1.0	16		0.0064	0.0329	0.1095	0.0727	-0.015	---	---	---	---	---	---	---	---	---	---	---	0.0064	0.0330	0.1109	0.1479	0.1219	---	---	---	---	---	---	---	---	---	---	---	---	---	
3	10	80		---	---	---	0.2397	0.6650	0.2910	0.9000	0.0110	---	---	---	---	---	---	---	---	---	---	---	0.2397	1.2263	0.0003	-0.117	0.1804	---	---	---	---	---	---	---	---	---	---	
4	100	400		---	---	---	0.2397	1.2263	0.2910	0.9000	0.0110	---	---	---	---	---	---	---	---	---	---	---	0.2396	1.1799	1.1659	9.4842	0.0110	---	---	---	---	---	---	---	---	---	---	---
True	Values			---	---	---	---	---	---	---	---	---	---	---	---	---	---	---	---	0.0064	0.0330	0.110	0.1480	0.1220	1.1800	0.1660	9.4842	0.0110	---	---	---	---	---	---	---	---	---	

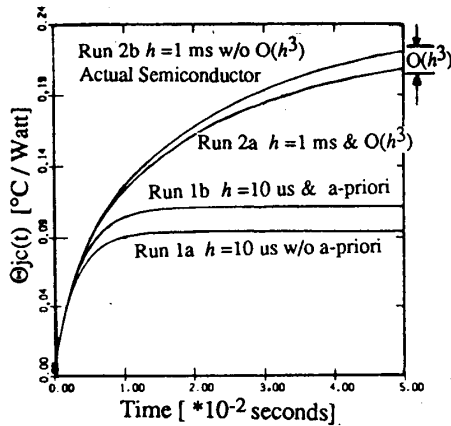


Fig. 10. Reconstructed versus actual TTIC's.

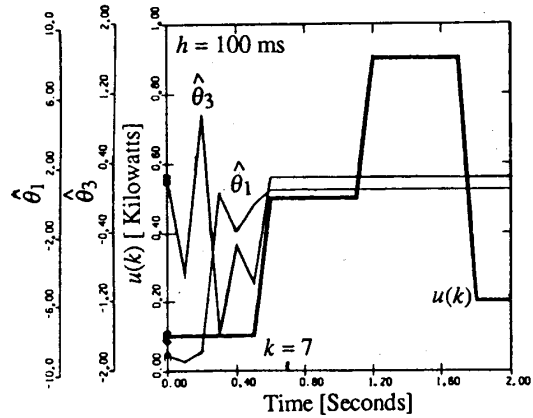


Fig. 12. Filter coefficient convergence for $u(k)$ input.

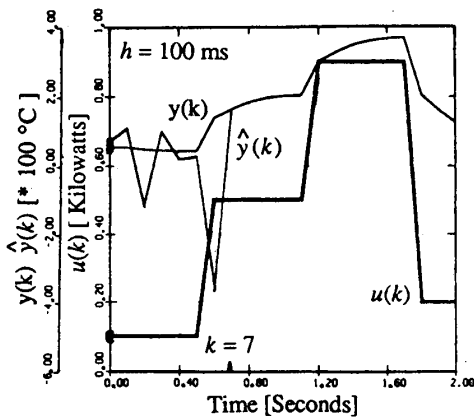


Fig. 11. $y(k)$ and $\hat{y}(k)$ response to $u(k)$.

istics was presented using system identification concepts. Governing thermal laws, device physical packaging construction, manufacturer's data specification sheet and standard TTIC graphical transfer function information were used as *a priori* knowledge to determine the model order and structure. The typical semiconductor model structure inherently contains wide time scale separation of the thermal time constants. This information was used to advantage in formulating a new systematic thermal RC Extraction procedure using RLS and time decoupled theory. Time decoupled theory used multiple RLS identi-

fication runs to estimate the major time constants in succession from the fastest to the slowest. The identified RC parameters from each run are found from the digital filter coefficients of the estimated mathematical transfer function $\hat{\Theta}_{jc}$. A test example using a transistor module was used to verify the proposed technique. Calculated RC parameters obtained from physical dimensions were also performed.

The proposed parameter identification concept may also be extended to other thermal systems with inherent overload capability such as transformers, rotating machines, etc. A TTIC curve can be generated for a step input of equipment power using output temperature data or possibly internal temperature states. However, a linearized model for a range of input power will be obtained due to nonlinear convection and radiation heat transfer. Time decoupled theory may possibly be extended to rotor time constant identification in ac vector control.

APPENDIX I
GOVERNING THERMAL LAWS

A RC parameter model of Fig. 1(c) and Fig. 5(d) is assumed for 50 A, 500 V, 300 W dual darlington isolated base transistor module with base dimensions of 1.25 × 3.6 inches. The specified $\Theta_{jc}(tss) = 0.41$ [°C/W] and has the TTIC curve shown in Fig. 6. Thermal resistance is directly analogous to Ohm's law for electrical resistance. A 45° angle from the junction to the case was assumed:

$$R_i = L_i / (K * Ae), \tag{39}$$

TABLE III
CALCULATED PARAMETER SPREADSHEET

Material	t (mils)	Ac (sq. inch)	Ae (sq. inch)	L _t	R _{ind} (C/W)	R _i (C/W)	C _i (W-s/C)
Silicon	15	0.43 x 0.43	0.43 x 0.43	= t/4 = t/4	0.008 0.008	0.008	0.033
Sn-Pb 10-90	3	0.43 x 0.43	0.43 x 0.43	= t	0.087	0.111	
Mo	20	0.43 x 0.43	0.43 x 0.43	= t/2 = t/2	0.016 0.016	0.122	0.148
Sn-Pb 75-25	17	0.43 x 0.43	0.43 x 0.43	= t	0.097	0.122	
Cu block	63	0.6 x 0.6	0.6 x 0.6	= t/2 = t/2	0.0089 0.0089	0.166	1.18
Sn-Pb 75-25	4	0.6 x 0.6	0.6 x 0.6	= t	0.012	0.166	
Al2O3	20	0.6 x 0.6	0.6 x 0.6	= t	0.109	0.166	
Sn-Pb 75-25	9	0.6 x 0.6	0.6 x 0.6	= t	0.027	0.166	
Cu base	118	1.2 x 1.2	0.75x0.75	= t/2 = t/2	0.010 0.010	0.010	9.50

TABLE IV
MATERIAL PROPERTIES ASSUMED

Material	K [W/(°C-in)]	ρ [lb/cu. in.]	C _p [W-s/lb-°C]
Silicon	2.134	0.083	303
280°C Solder (Sn10-Pb90)	0.914	—	—
Molydendum 180°C Solder (Sn75-Pb25)	3.296	0.369	115
Ceramic	0.914	—	—
Copper	0.510	—	—
	9.77	0.320	175

L_t = thickness [inch] of material along heat flow path;

K = material thermal conductivity from Table IV;

Ae = cross section area [sq. in.] perpendicular to heat flow path;

in calculating an effective heat spreader area {Ae} for succeeding layers with a much greater true cross sectional area {Ac}. Thermal resistance {R_t} is calculated to the midpoint of each major heat capacity material where the capacitance {C_i} is assumed a lumped parameter. However, the silicon chip is an exception where it is assumed that the top 1/2 of the thickness {L_t} is really the distributed power source {P}. The ceramic insulator (26%) and solder interfaces (34%) account for 50% of the specified Θ_{jc} (tss).

The thermal capacitance is calculated using true material volume:

$$C_i = \rho * C_p * V, \quad (40)$$

ρ = density of the material from Table IV,

C_p = specific heat of the material from Table IV,

V = true material volume (L_t * Ac) [in³].

APPENDIX II

DISCRETE TRANSFER FUNCTION MODEL

Let the following constants be defined for a chosen sample time h:

$$K_{11} = h/R_1 C_1 \quad K_{21} = h/R_2 C_1$$

$$K_{22} = h/R_2 C_2 \quad K_{32} = h/R_3 C_2$$

$$\Phi = \begin{pmatrix} (1 - K_{11}) K_{21} \\ K_{22} \quad (1 - K_{22} - K_{33}) \end{pmatrix}$$

$$\Gamma = (h/C_1) * \begin{pmatrix} (1 - 0.5 * K_{21}) \\ 0.5 * K_{22} \end{pmatrix}$$

$$C = [1 \ 0] \quad D = [R_1]$$

The digital filter coefficients used in (18) transfer function are

$$a_1 = -2.0 + K_{21} + K_{22} + K_{32}$$

$$a_2 = 1.0 - K_{21} - K_{22} - K_{32} + K_{21} * K_{32}$$

$$b_0 = R_1$$

$$b_1 = R_1 \{-2.0 + K_{11} + K_{21} + K_{22} + K_{32} - 0.5 * K_{11} * K_{21}\}$$

$$b_2 = R_1 \{1.0 - K_{11} - K_{21} - K_{22} - K_{32} + 0.5 * K_{11} * K_{21}$$

$$+ \dots K_{11} * K_{22} + K_{11} * K_{32} + K_{21} * K_{32} - O(h^3)\}$$

where the O(h³) = 2nd order error term = 0.5 * K₁₁ * K₂₁ * K₃₂.

ACKNOWLEDGMENT

The author's wish to thank Wisconsin Alumni Research Foundation (WARF) and K. Phillips, J. VanderMeer of Eaton for project support, and Prof. D. Divan and S. Bhattacharya for helpful suggestions.

REFERENCES

- [1] F. Gutzwiller and T. Sylvan, "Power semiconductor ratings under transient and intermittent loads," in *Rec. AIEE Winter Meeting*, 1959.
- [2] P. Hower, D. Blackburn, F. Ottinger, and S. Rubin, "Stable hot spots and second breakdown in power transistors," in *IEEE Power Electronics Specialist Conf. Rec.*, 1976.
- [3] R. Chick, "How to power rate a transistor," *Solid State Power Conv.*, Mar./Apr. 1977.
- [4] "Transistor safe operating area," Amperex Report S169, 1981.
- [5] W. C. Schultz, "Power transistor safe operating area," *Power Conversion International*, July/Aug. 1982.
- [6] R. Prest and J. Van Wyk, "Improved dc modeling of high current bipolar transistors for accurate converter simulation," in *IEEE IAS Annual Conf. Rec.*, 1989, p. 1235.
- [7] S. Menhart and W. Portnoy, "Development of a secondary breakdown model for bipolar transistors," in *IEEE IAS Annual Conf. Rec.*, 1989, p. 1243.
- [8] G. Skibinski, W. Sethares, and D. Divan, "Adaptive current regulators to maximize overload capability," Wempec notes.
- [9] K. Astrom and P. Eykhoff, "System identification—A survey," in *2nd IFAC Symp. Identification and Process Parameter Estimation Rec.*, 1970; also in *Automatica*, vol. 7, pp. 123-162, 1971.
- [10] I. Gustavson, "Survey of applications of identification in chemical and physical processes," in *3rd IFAC Symp. Identification and System Parameter Estimation Rec.*, 1973.
- [11] F. Ottinger, D. Blackburn, and S. Rabin, "Thermal characterization of power transistors," *IEEE Trans. Electron Devices*, vol. ED-23, 1976.
- [12] "Thermal resistance measurements of conduction cooled power transistors," EIA Standard RS-313-13, 1975 Electronic Industry Association, 2001 Eye Street, N.W., Washington, DC 20006.
- [13] K. Astrom and Wittenmark, *Computer Controlled Systems*. Englewood Cliffs, NJ: Prentice Hall, 1984.
- [14] S. Wolfram, *Mathematica*. Reading, MA: Addison-Wesley, 1988.

- [15] C. Johnson, *Lectures on Adaptive Parameter Estimation*, Lecture 5, "Persistent excitation and parameter convergence." Englewood Cliffs, NJ: Prentice Hall, 1988.
- [16] *ACSL Ref. Manual*, Mitchell & Gauthier Assoc., Concord, MA.
- [17] B. D. O. Anderson, R. R. Bitmead, C. R. Johnson, Jr., P. V. Kokotovic, R. L. Kosut, I. M. Y. Mareels, L. Praly, and B. D. Reidle, *Stability of Adaptive Systems: Passivity and Averaging Analysis*. Cambridge, MA: MIT Press, 1986.
- [18] S. Haykin, *Adaptive Filter Theory*. Englewood Cliffs, NJ: Prentice-Hall,

Project Engineer working on a real time data acquisition motor dynamometer laboratory. From 1982 to 1985 worked as Senior Project Engineer on design and analysis of dc and ac servo controllers. In 1985 he was appointed Principal Engineer at RTE Corporation R & D working on UPS and switching supply topologies. His present interest is investigating new power electronic converter technologies.

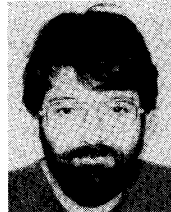
Mr. Skibinski is a member of Phi Kappa Phi and Tau Beta Pi. He is a Professional Engineer in the State of Wisconsin and the recipient of two Prize Paper awards at the 1987 and 1990 IEEE IAS Annual Conferences.



Gary L. Skibinski was born in West Allis, WI in 1953. He received the B.S.E.E. and M.S.E.E. degrees from the University of Wisconsin-Milwaukee in 1979 and 1980, respectively. He is currently a Ph.D. candidate at the University of Wisconsin-Madison.

He joined Eaton Corporation in 1976 as a Design Engineer in the Solid State Power Conversion Lab where he has worked on the design of a voltage source inverter propulsion drive for a Navy minisubmarine, a static rod drive system for Navy nuclear reactors, and a commercial current source inverter drive. He joined Allen Bradley Corporate R & D in 1980 as a

Project Engineer working on a real time data acquisition motor dynamometer laboratory. From 1982 to 1985 worked as Senior Project Engineer on design and analysis of dc and ac servo controllers. In 1985 he was appointed Principal Engineer at RTE Corporation R & D working on UPS and switching supply topologies. His present interest is investigating new power electronic converter technologies.



William A. Sethares (S'84-M'86-S'86-M'87) received the B.A. degree in mathematics from Brandeis University, Ithaca, NY.

He has worked at the Raytheon Company as a Systems Engineer and is currently with the Department of Electrical and Computer Engineering at the University of Wisconsin in Madison. His research interests include adaptive systems, and applications of system identification techniques to control, power, and semiconductor processes.